Electronic Supplementary Material (ESI) for RSC Advances.

Hierarchical $NaFePO_4$ nanostructures in combination with optimized carbon-based electrode to achieve advanced aqueous Na-ion supercapacitors

Sudipta Biswas[a], Debabrata Mandal[b], Trilok Singh[c] and Amreesh Chandra[a,b,d]

[a]*Department of Physics, Indian Institute of Technology Kharagpur, Kharagpur-721302*

[b]*School of Nano Science and Technology, Indian Institute of Technology Kharagpur, Kharagpur-721302*

[c] *Functional Materials and Device Laboratory, School of Energy Science & Engineering, Indian Institute of Technology Kharagpur, Kharagpur-721302*

[d] *School of Energy Science & Engineering, Indian Institute of Technology Kharagpur, Kharagpur-721302*

Synthesis of carbon structures:

1.1 Activated carbon

Activated carbon was purchased from Merck Industries Pvt. Ltd. and used without any treatment.

1.2 Carbon microsphere

Dextrose was used as a carbon source by the hydrothermal method to synthesize the carbon sphere. The size of the particle can be controlled by controlling the amount i.e., the molarity of dextrose present in the solution. Suitable synthesis temperature is required to disintegrate carbon from the dextrose. The duration of hydrothermal treatment was varied. 100 ml, 1 M transparent dextrose solution was prepared and transferred to a Teflon lined autoclave (300 mL) so that it fills one-third of the volume. The autoclave was then tightly sealed and heated at 160 °C for 6 h in an oven. The hydrothermal chamber was allowed to cool down at room temperature after the heating procedure. The obtained brownish product was washed four times with DI water, followed by ethanol three times. Finally, the black powder was dried at 65 °C overnight.

1.3 Carbon nanosphere

The carbon microspheres were synthesized by the hydrothermal synthesis route. In brief, 6 grams of dextrose was dissolved in 60 ml of DI water. Then 5 mg of CTAB was added in the above solution. The mixture was then transferred into a Teflon sealed stainless steel autoclave and maintained at 180 ºC for 10 h. The black product was filtered and washed several times with DI water and acetone. Finally, the obtained material was oven-dried for 6 h at 80 ºC.

1.4 Graphene Oxide (GO)

GO was synthesized using a modified Hummer's methods. Initially, graphite powder was added into sulfuric acid (98%) in an ice bath. Potassium permanganate was gradually added into this mixture. Following stirring for 10 min, sodium nitrate was added. This solution was

further stirred for 3 h at 35 ºC before dilution by deionized (DI) water. The reaction was terminated by the addition of H_2O_2 (30%). The obtained light yellow color graphite oxide was washed with dilute HCl (volume ratio of 1:10 for HCl to DI water) to remove the residual ions. Finally, the suspension was filtered and washed with DI water several times till pH~7 was obtained. The brown-colored aqueous graphite oxide suspension was sonicated for 40 min for exfoliation. Finally, the sonicated suspension was centrifuged at 3500 rpm for 30 min.

1.5 Reduced graphene oxide (rGO)

GO was reduced by $NaBH_4$. In a typical reduction, GO (0.6 g) was stirred in 200 ml pure water and was dispersed finely in water by ultrasonic bath for 3 h. Then, while the GO suspensions were stirred, $NaBH_4$ (2 g) was added to the GO suspension. The suspension was heated by a hot plate. The solution was heated in an oil bath at 80-100 °C under a water-cooled condenser or without condenser for 12 and 24 h. The water level was kept during all the reductions. RGO's were precipitated by centrifugation or filtration. Then, precipitated RGO samples were washed with acetone and pure water and ethanol. Finally, correctly cleaned and precipitated RGOs were dried in an oven with or without a vacuum.

1.6 Graphene Quantum Dot (GQD)

The GQDs were prepared by the pyrolysis of Citric Acid. This is a simple bottom-up method to process GQDs, in this process 2 g Citric Acid was put into a 10 mL beaker and heated to 200 °C continuously for 10 min, after that Citric Acid became liquid, and the color of the liquid was changed from colorless to pale yellow, and then orange in 25 min, it indicated the formation of GQDs. The obtained orange GQDs was added drop by drop into 100 mL of 10 mg mL^{-1} NaOH solution, under vigorous stirring and further neutralized to pH 7.0 with NaOH, the aqueous solution.

1.7 Nitrogen-doped Graphene Quantum Dot (nGQD)

The GQDs were prepared by the pyrolysis of Citric Acid. This is a simple bottom-up method to process GQDs, in this process 2 g Citric Acid was put into a 10 mL beaker and heated to 200 °C continuously for 10 min. After the Citric Acid became liquid, its color was changed from colorless to pale yellow, followed by orange in 25 min, indicating the formation of GQDs. The obtained orange GQDs were added dropwise into 100 mL of 10 mg mL^{-1} NH_3 solution, under vigorous stirring, and neutralized to pH 7.0 to form NGQDs.

2.0 Synthesis of $NaFePO_4$:

Porous and hollow $NaFePO_4$ microstructures were synthesized using a one-pot facile hydrothermal route followed by calcination in air. In a typical experimental procedure, 25 ml of 0.1 M ferric nitrate solution was mixed with 25 ml of 0.1 M stearic acid solution. Subsequently, 245.1 mg trisodium citrate ($Na_3C_6H_5O_7$, $2H_2O$) was added, and the solution was stirred for 2 h. An appropriate amount of ammonium dihydrogen phosphate ($(NH_4)H_2PO_4$) was added to the precursor solution so as to ensure Na:Fe:PO_4 concentration ratio was 1:1:1. 50 ml of this yellow-colored solution was then transferred to Teflon-lined stainless steel (capacity 250 ml) autoclave. The autoclave was kept at 180 ºC for 24 h, before allowing it to slowly cool down to the room temperature. The precipitate was collected by centrifugation at 3200 rpm. The precipitate was subsequently washed three times using de-ionized water and dried overnight in a vacuum oven at 70 ºC. The dried sample was crushed and annealed at 600 ºC for 4 h in the air to obtain hollow $NaFePO_4$ powder.

Characterization:

The phase formation of the synthesized materials was confirmed by analyzing the powder x-ray diffraction (XRD) profiles using Rigaku miniflex 600 diffractometer with Cu-Kα (lambda = 0.15406 nm) as an excitation wavelength in 2θ range 5-70°. Scanning electron microscopy (SEM CARL ZEISS SUPRA 40) and transmission electron microscopy (TEMFEI-TECHNAI G220S-Twin operated at 200 kV) were used for morphological analysis of the obtained sodium-based phosphate and carbon structure. The Brunauer-Emmett-Teller (BET) surface area and pore size were estimated by analyzing N_2 adsorption-desorption isotherms studied by Quantachrome Nova touch surface area and pore size analyzer. Zeta potential and particle size of the samples were measured by using Horiba Scientific Nano Particle Analyzer SZ-100.

Growth mechanism of the hollow $NaFePO_4$ structures:

In an autoclave container under high pressure, the reagents react and formed a spherical particle via kinetically controlled diffusion with the help of self-assembled stearate ion template. Then these spherical particles are washed and dried at 70 °C. The synthesized spherical particles then calcined at 4 h under air ambient to remove unwanted gaseous products and this process leads the formation of hollow as well as porous structures.

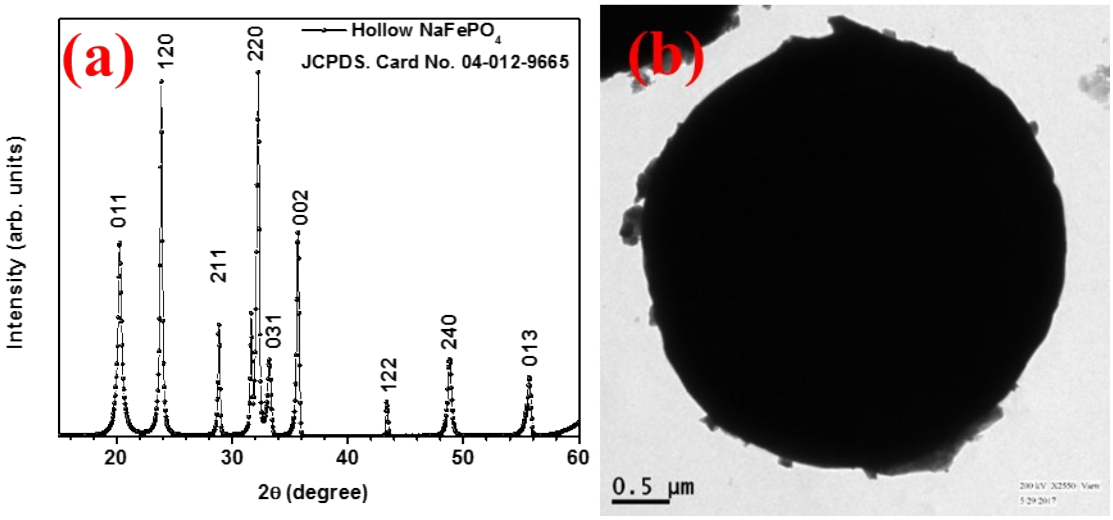

Fig. S1 (a) *XRD profiles and (b) TEM micrographs of hollow $NaFePO_4$ structures.*

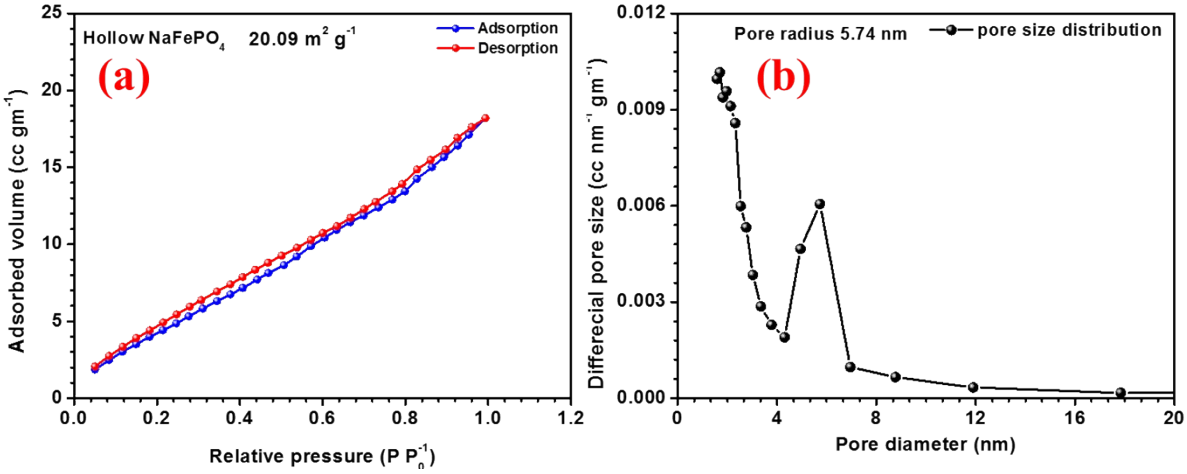

Fig. S2 (a) N_2 adsorption desorption graph and (b) pore size distribution of hollow $NaFePO_4$ structures.

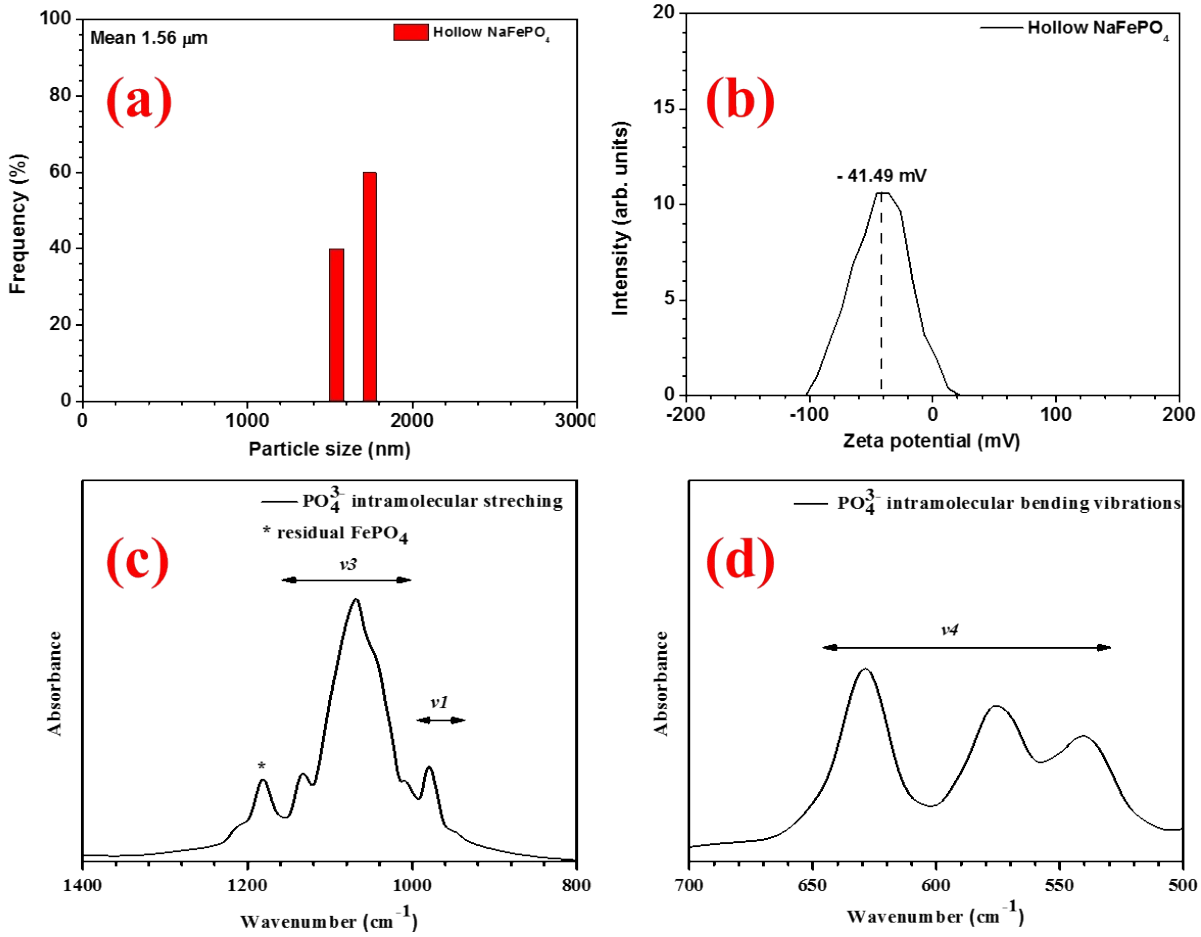

Fig. S3 (a) particle size distribution, (b) zeta potential distribution, (c, d) FTIR spectra of $NaFePO_4$.

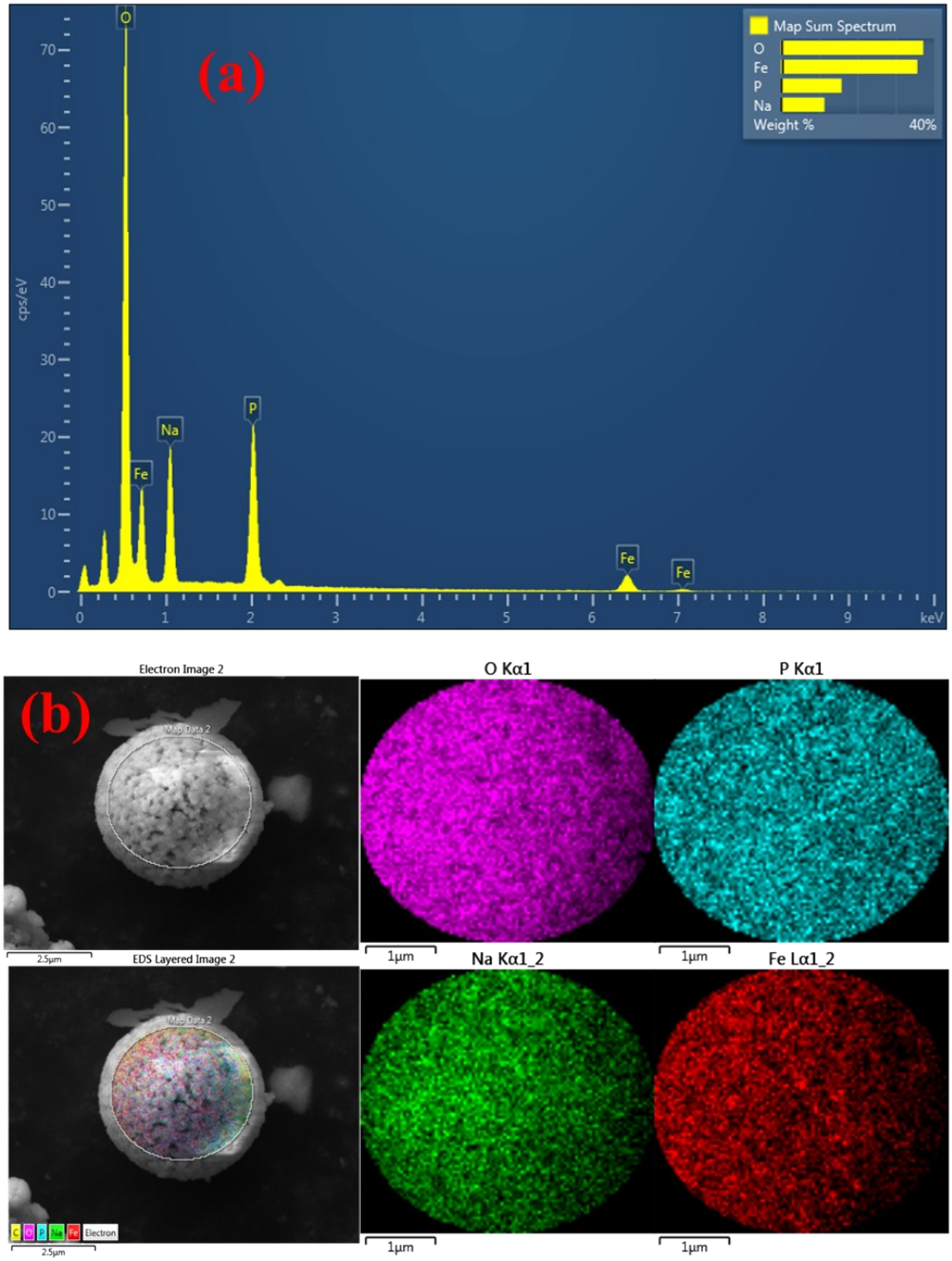

Fig. S4 (a) EDAX spectra and (b) elemental mapping of the hollow $NaFePO_4$ sphere.

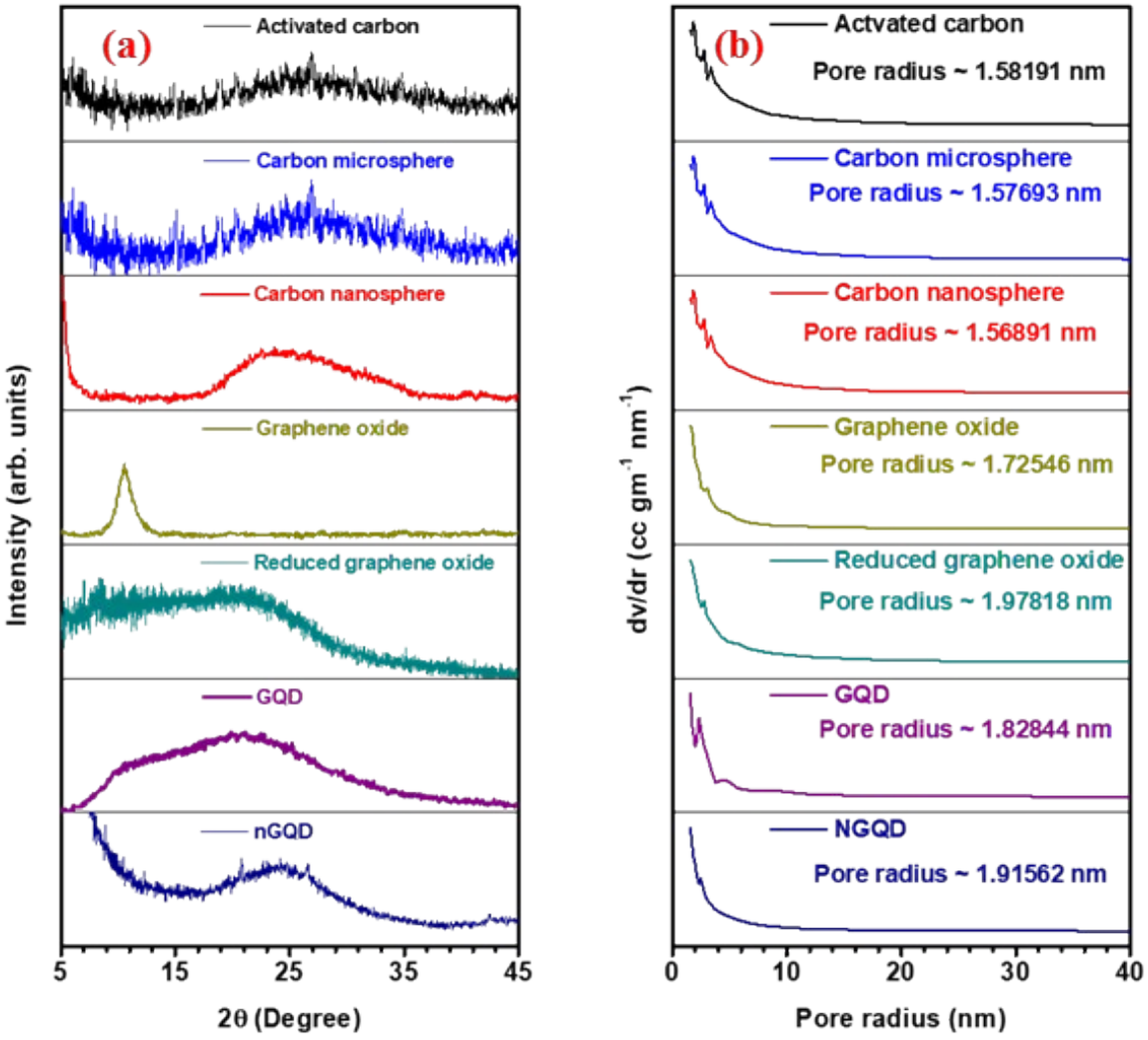

Fig. S5 *(a) XRD profiles and (b) pore size distribution for the different carbon structures: activated carbon, carbon microsphere, carbon nanosphere, graphene oxide, reduced graphene oxide, graphene quantum dot and nitrogen doped graphene quantum dot, respectively.*

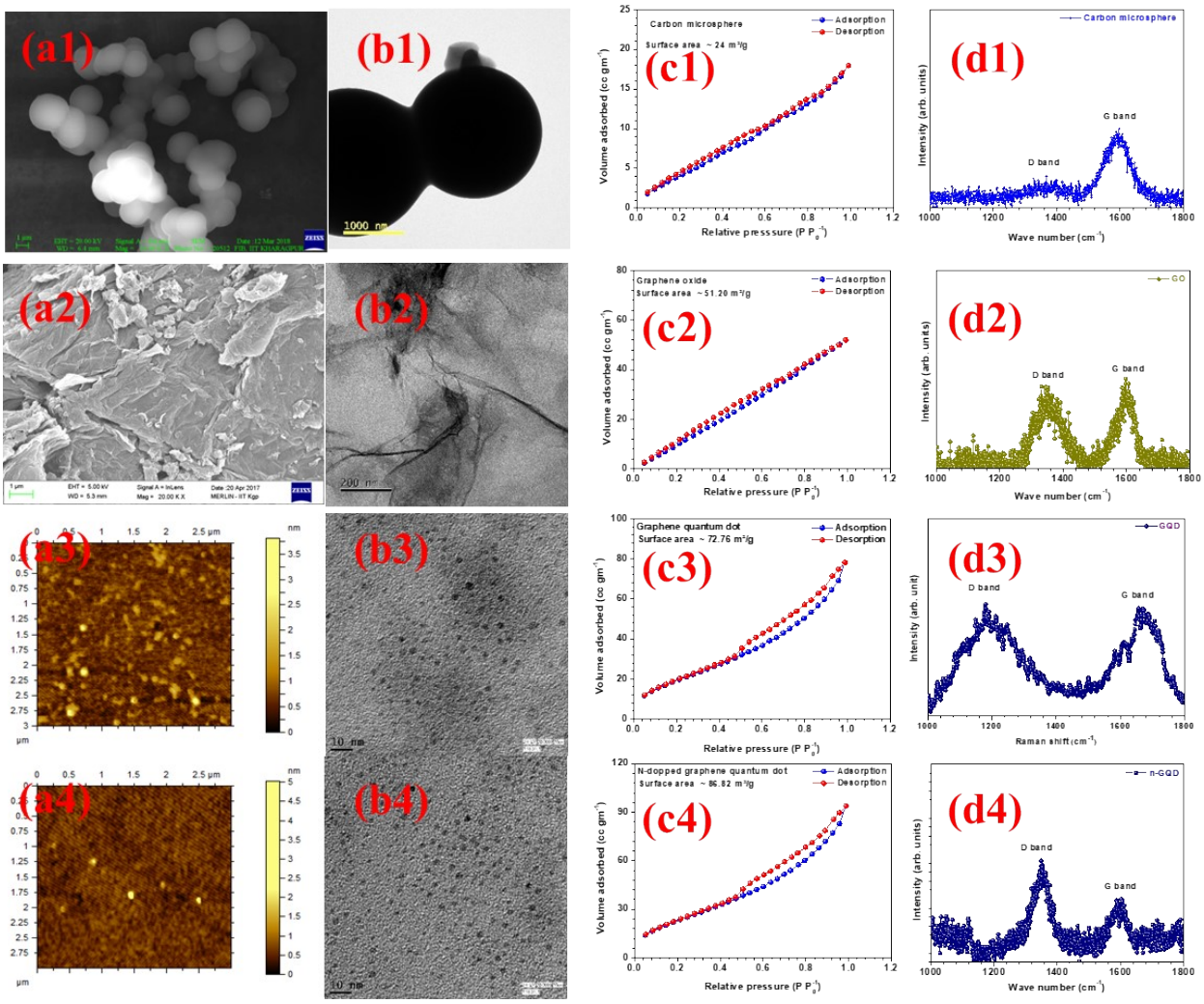

Fig. S6 (a1-a2) SEM for CMS, GO; (a3-a4) AFM for GQD and nGQD; (b1-a4) TEM and (c1-c4) BET isotherm for CMS, GO, GQD, nGQD and (d1-d4) Raman spectra, respectively.

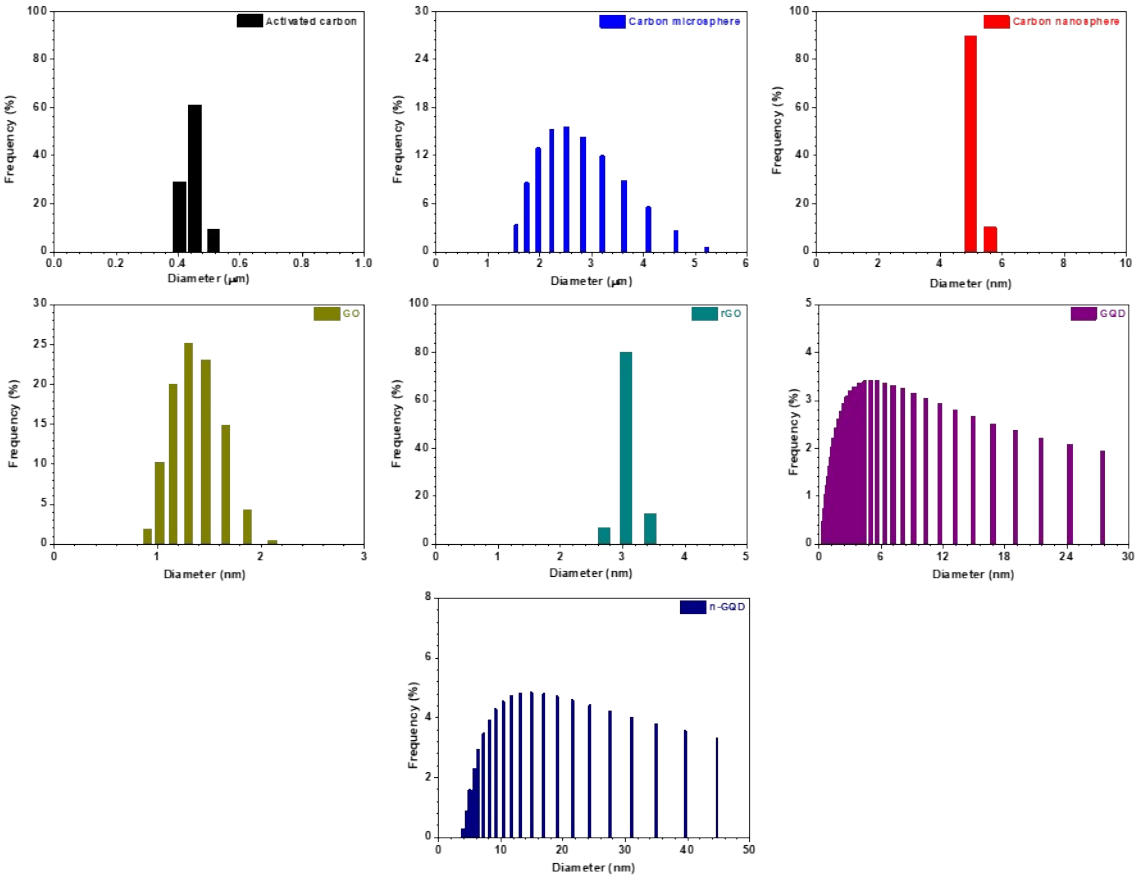

Fig. S7 (a-g) Particle size distribution for AC, CMS, CNS, GO, rGO, GQD and nGQD, respectively.

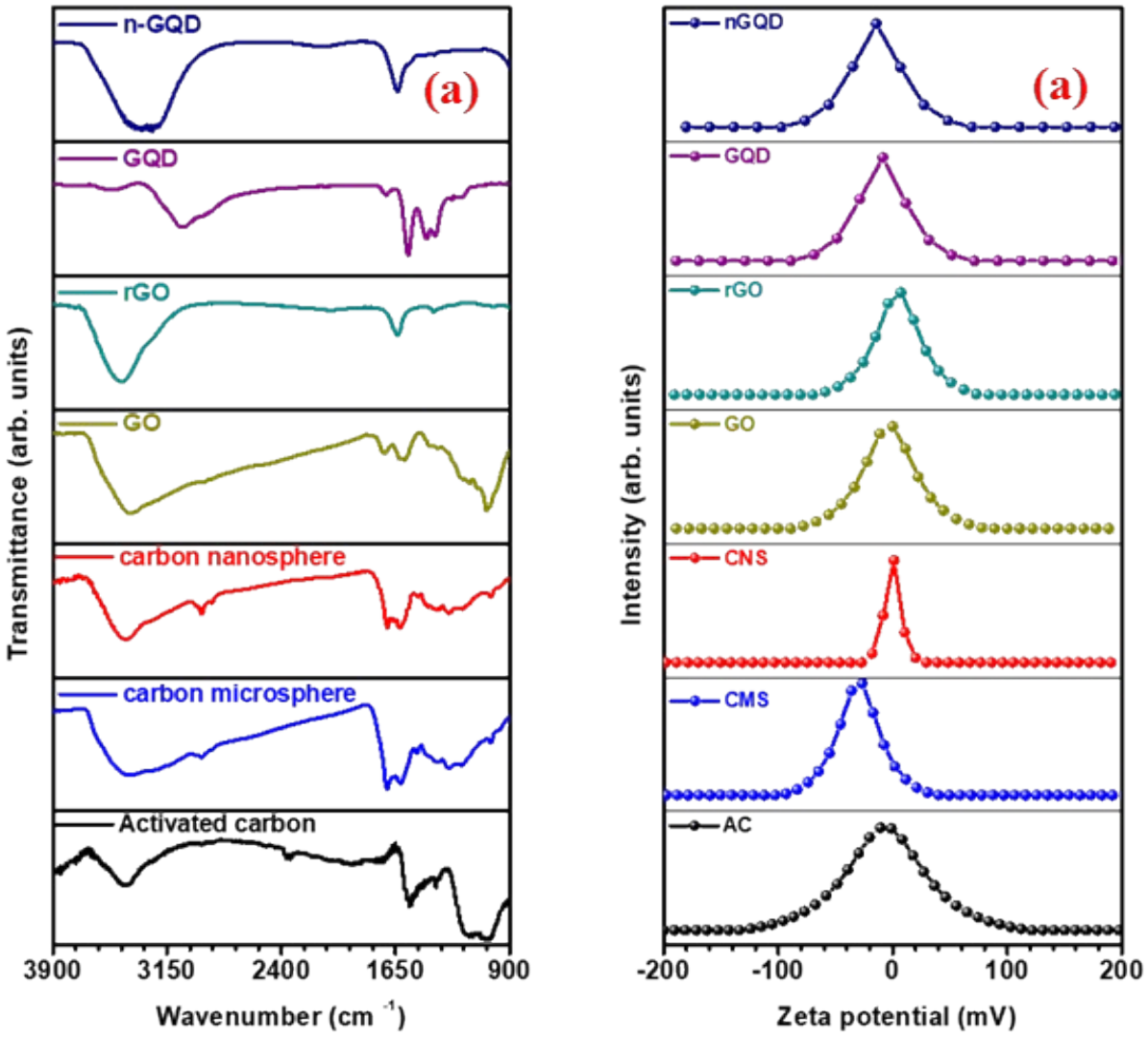

Fig. S8 (a) FTIR spectra and (b) Zeta potential values for the carbon structures.

FTIR spectra for all the carbon structures are shown in Fig. S6(a). The FTIR spectrum of the GO sample has shown various oxygen configurations in the structure includes the vibration modes of epoxide (C-O-C) (1230-1320 cm^{-1}), sp^2-hybridised C=C (1400 cm^{-1}, in-plane vibrations), carboxyl (COOH) (1650-1750 cm^{-1} including C-OH vibrations at 3530 and 1080 cm^{-1}), ketonic species (C=O) (1725 cm^{-1}) and hydroxyl (namely phenol, C-OH) (3690 cm^{-1}) with all C-OH vibrations from COOH and H_2O[28]. The FTIR spectrum of the rGO sample showed no signature peak of OH group around ~ 3338 cm^{-1} indicating complete conversion of carbon into the rGO[29]. The absorption peak 1568 cm^{-1} indicates the presence of C=C and the absorption peak 1164 cm^{-1} indicates C-OH group. FTIR obtained for GQDs exhibit absorption of a carboxyl group and a hydroxyl group, both materials contain -COOH groups and -OH groups. GQDs showed absorption of stretching vibration C–H at 2950 cm^{-1} and stretching vibration of C–H in the range below 1350 cm^{-1}, suggesting that the GQDs contain some carbonized Citric acid[10]. In the FTIR spectra shown in Fig.S6, the characteristic absorption bands stretching vibration of C–H in aromatic rings are around 3000–3100 $cm^{-1}$and vibration of aromatic rings are around 1450–1650 cm^{-1} for GQDs[30]. The peaks at1178 cm^{-1} and 1231 cm^{-1} are indicated to the stretching vibration bonds of C–OH in NGQDs. The absorption peak at 1376 cm^{-1} is the stretching vibration bond of C-NH in N-GQDs and 1706 cm^{-1} is the characteristic peak of C=O groups on the surface of NGQDs. The peak at 3062 cm^{-1} could be indicated the stretching vibration of N-H in NGQDs[31]. The zeta potential values obtained for AC, CMS, CNS, GO, rGO, GQD, NGQDs are -6.61, -29.76, -0.07, -3.20, 4.43, -9.31 and -14.25 mV respectively, as shown in Fig. S6(b). CMS showed the lowest zeta potential value, which also corroborates the corresponding surface area for the material to be lowest among all.

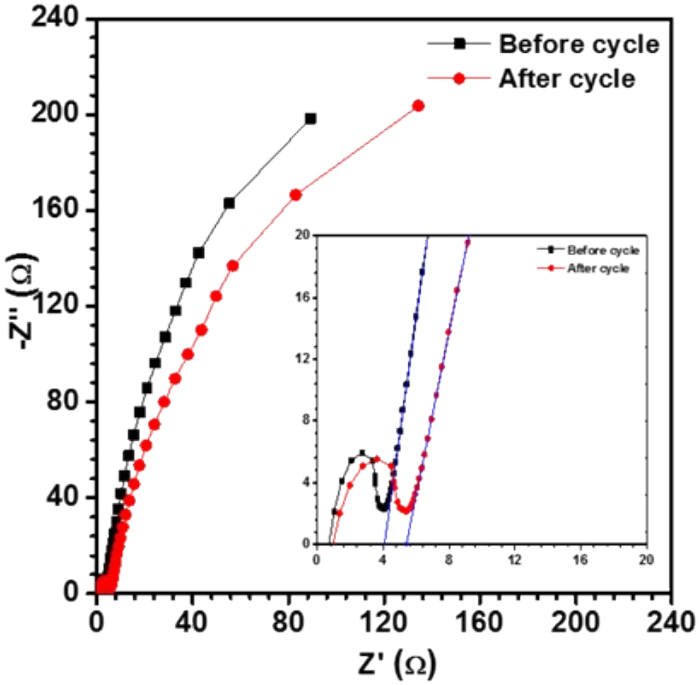

Fig. S9 ESR spectroscopy for electrodes with hollow $NaFePO_4$ structures.

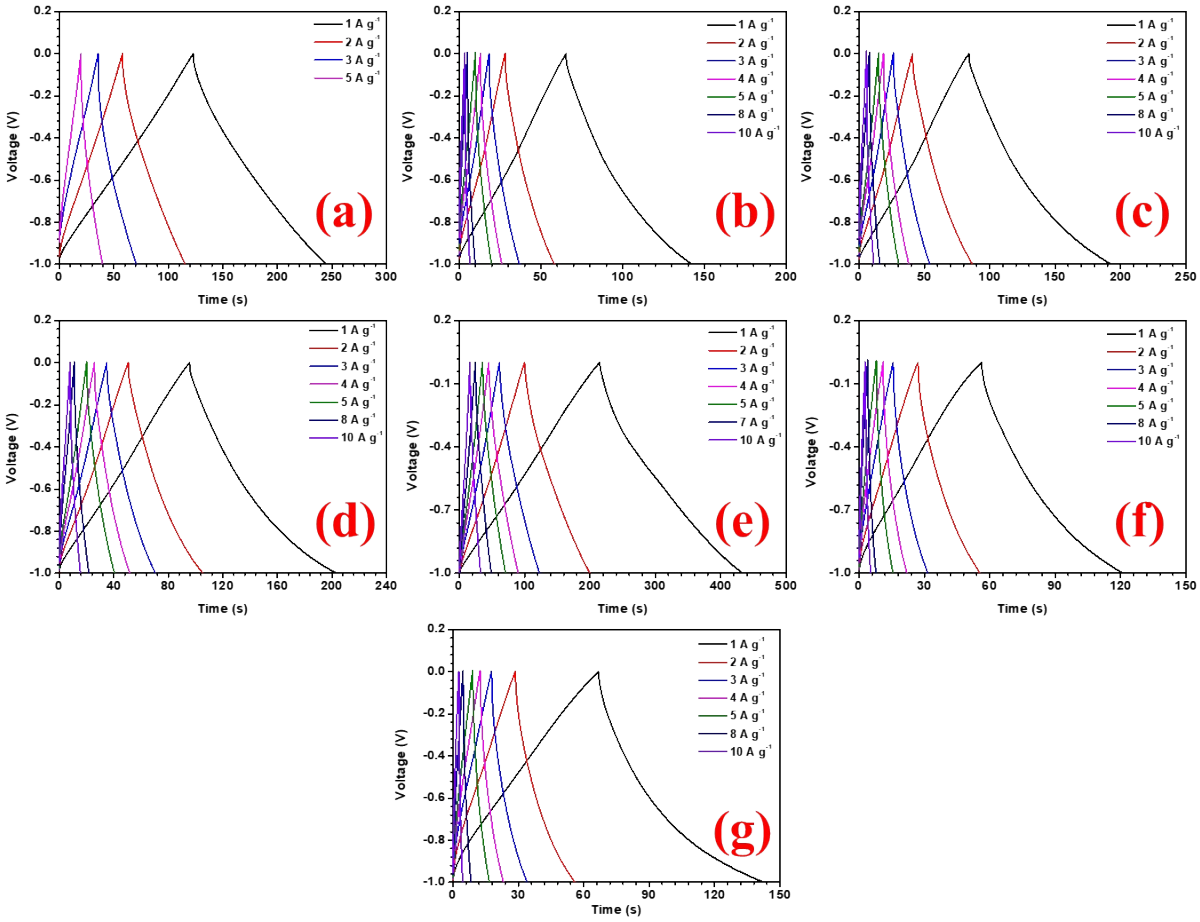

Fig. S10 CD profiles at different scan rates (a) activated carbon, (b) carbon microsphere, (c) carbon nanosphere, (d) graphene oxide (GO), (e) reduced graphene oxide (RGO), (f) graphene quantum dot (GQD) and (g) nitrogen doped graphene quantum dot (NGQD).

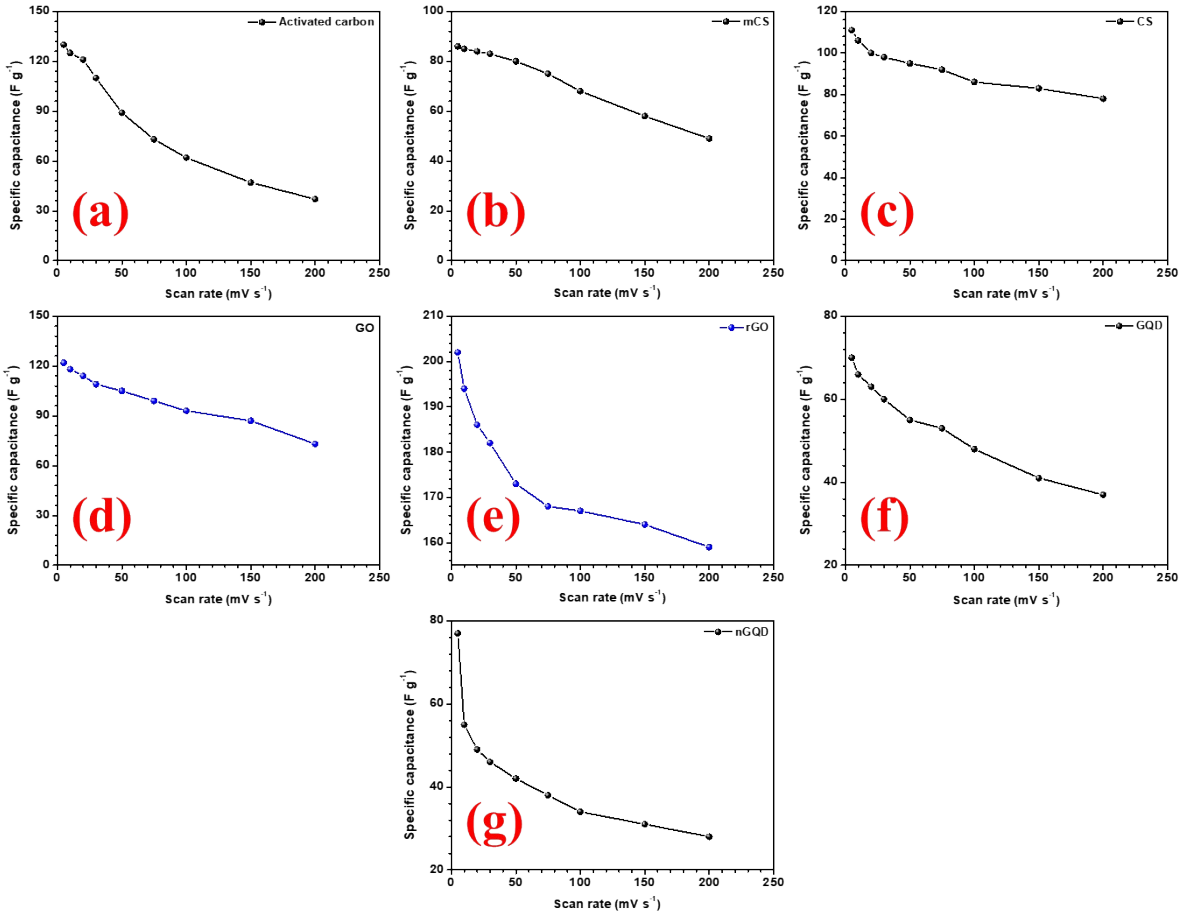

Fig. S11 Variation of specific capacitance with scan rates for (a) activated carbon, (b) carbon microsphere, (c) carbon nanosphere, (d) graphene oxide (GO), (e) reduced graphene oxide (RGO), (f) graphene quantum dot (GQD) and (g) nitrogen doped graphene quantum dot (NGQD).

The relation used for calculation of the average specific capacitance in three-electrode setup from the CV curves for the single electrode is:

$$C_{CV} = \frac{1}{2mv \triangle V} \int_{-V}^{+V} I.dV \quad (1)$$

where m, v, ΔV and $\int_{-V}^{+V} I.dV$ denote the mass of the active material, scan rate, potential window, and absolute area under the CV loop, respectively.

The results from the CV profiles in the three-electrode system are also supported by the charge-discharge (CD) measurement, which is shown in Fig. S6. The specific capacitance values are calculated using the relation

$$C_{CD} = \frac{I.dt}{m.(V - IR)} \quad (2)$$

where, I/m, dt, V, and IR denotes the current density, time of discharge, voltage window, and the voltage drop during discharge, respectively.

The specific capacitance for the device from the CV curves is calculated using the relation:

$$C_{CV} = \frac{1}{mv \triangle V} \int_{-V}^{+V} I.dV \quad (3)$$

where m, v, ΔV and $\int_{-V}^{+V} I.dV$ denote the mass of the active material, scan rate, potential window, and absolute area under the CV curve, respectively.

The specific capacitance values for the device is calculated using the relation

$$C_{CD} = \frac{I.dt}{m.(V - IR)} \quad (4)$$

where, I/m, dt, V, and IR denotes the current density, time of discharge, voltage window, and the voltage drop during discharge, respectively.

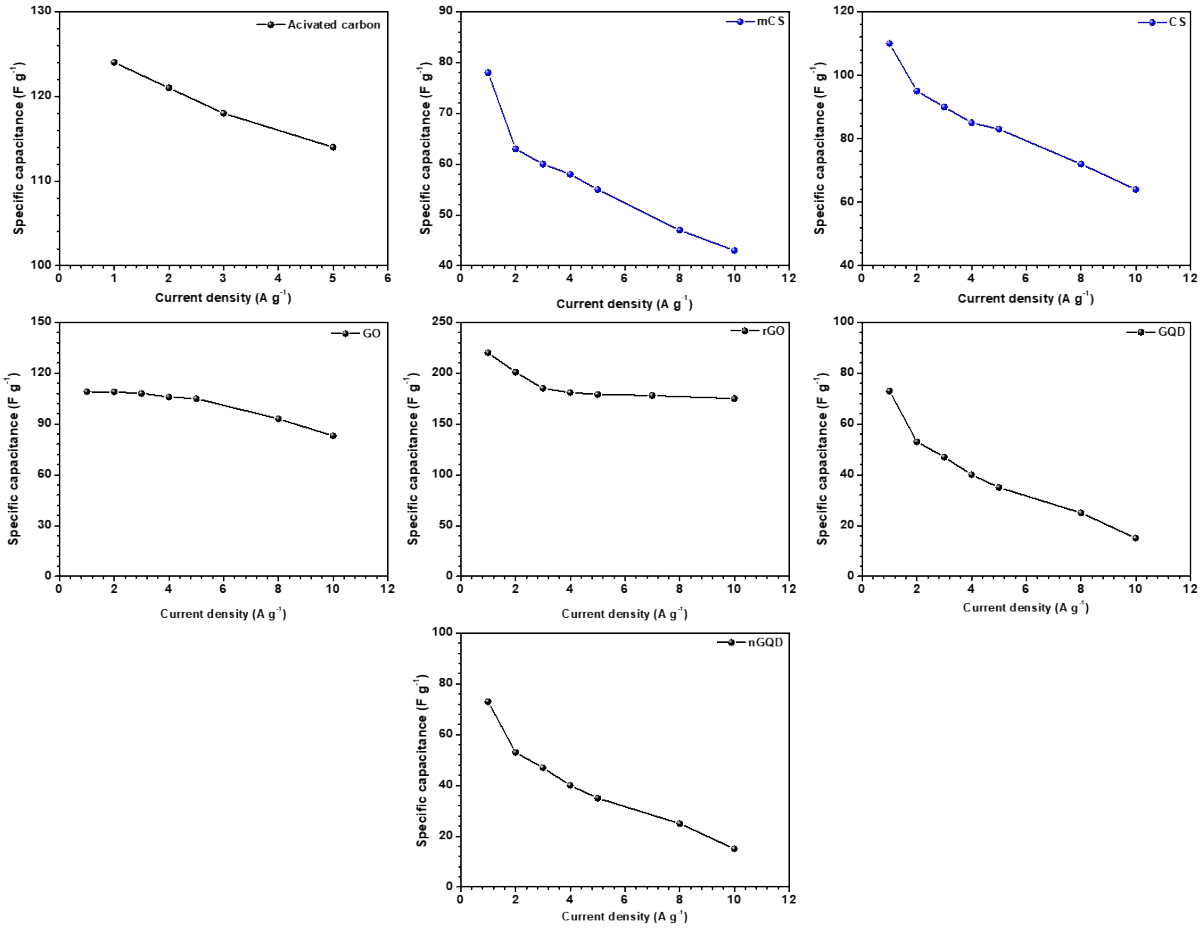

Fig. S12 Variation of specific capacitance with current densities for (a) activated carbon, (b) carbon microsphere, (c) carbon nanosphere, (d) graphene oxide (GO), (e) reduced graphene oxide (RGO), (f) graphene quantum dot (GQD) and (k,l) nitrogen doped graphene quantum dot (NGQD).

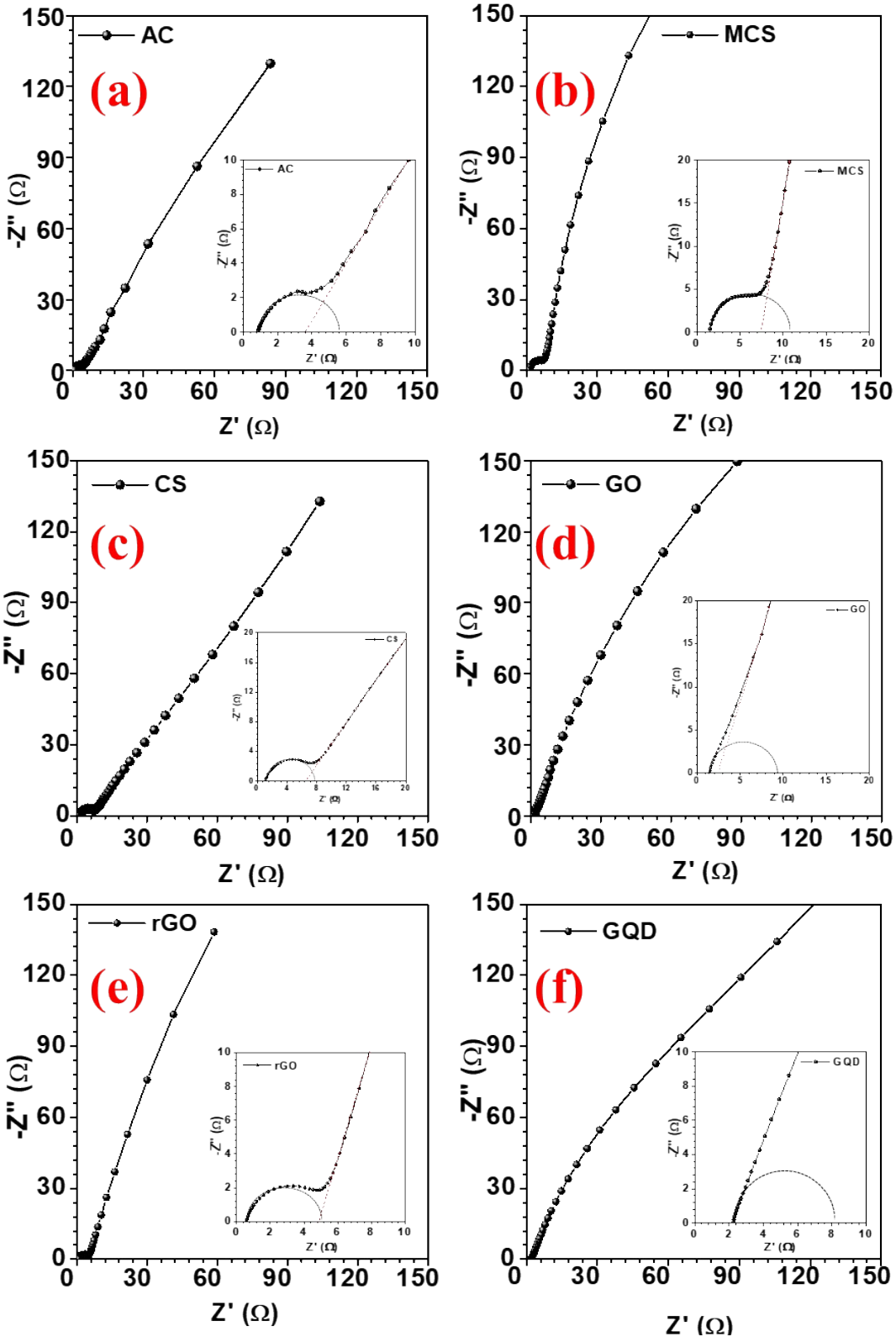

Fig. S13 Nyquist plots for (a) activated carbon, (b) carbon microsphere, (c) carbon nanosphere, (d) graphene oxide (GO), (e) reduced graphene oxide (RGO), (f) graphene quantum dot (GQD) and (k,l) nitrogen doped graphene quantum dot (NGQD).

Table S1. Values of ESR, Warburg resistance and charge transfer resistance for all the carbon structures in the 3-electrode measurement.

Material	Scan rate (mV/s)	ESR (R_s in Ω)	Warburg resistance (W_s in Ω)	Specific Capacitance (F g⁻¹)	Charge transfer resistance (R_{ct} in Ω)
AC	5	0.90	3.69	108	4.28
MCS	10	1.49	7.43	106	8.33
CS	20	1.07	6.47	95	7.35
GO	30	1.51	2.42	94	9.38
RGO	50	0.59	4.89	78	1.83
GQD		2.22	--		--
N-GQD		1.97	--		--

Table S3. Specific capacitance of hollow and porous $NaFePO_4$ form CD curves in 2 M NaOH electrolyte

Table S2. Specific capacitance of hollow and porous $NaFePO_4$ form CV curves in 2 M NaOH electrolyte

Current Density ($A\,g^{-1}$)	Specific capacitance ($F\,g^{-1}$)
1	115
2	106
3	96
5	66

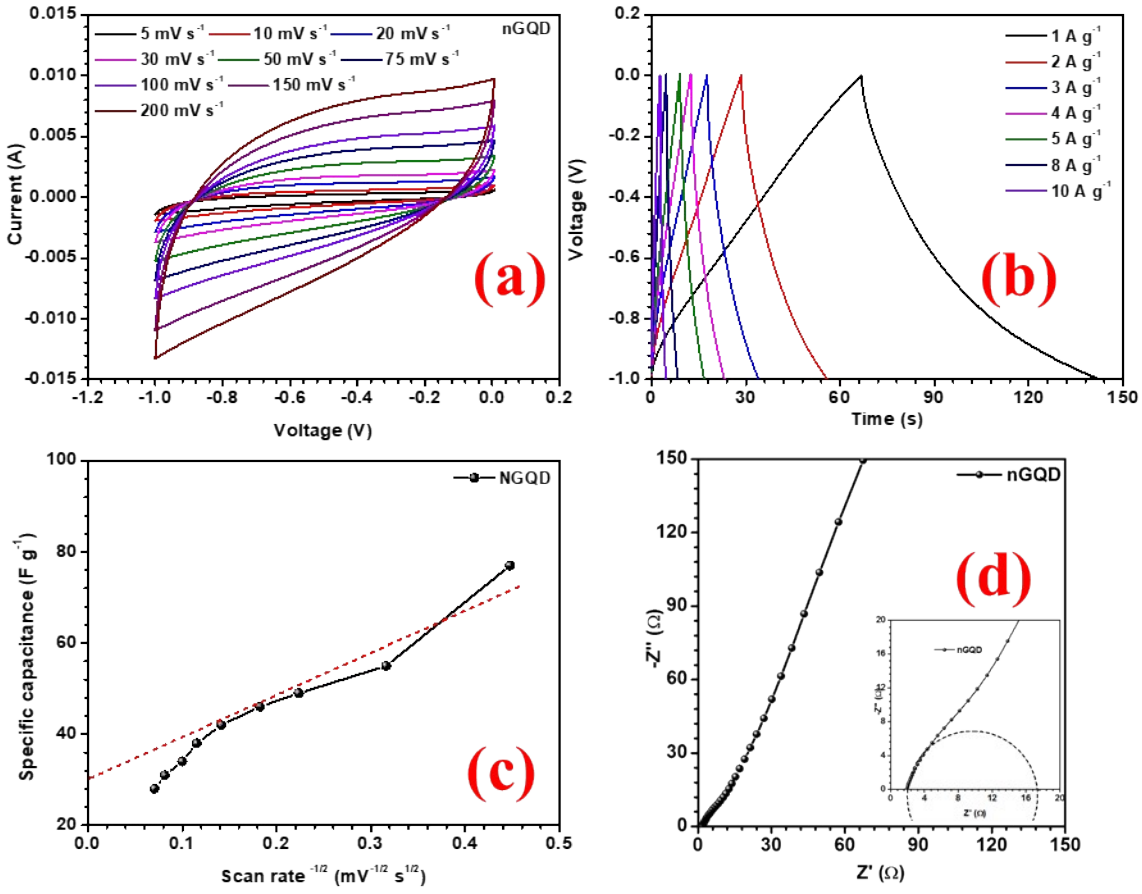

Fig. S14 (a) CV profiles at different scan rate, (c) charge discharge at different current density, (c) specific capacitance with inverse of the scan rate and, (d) variation of specific capacitance with current density for NGQD electrode.

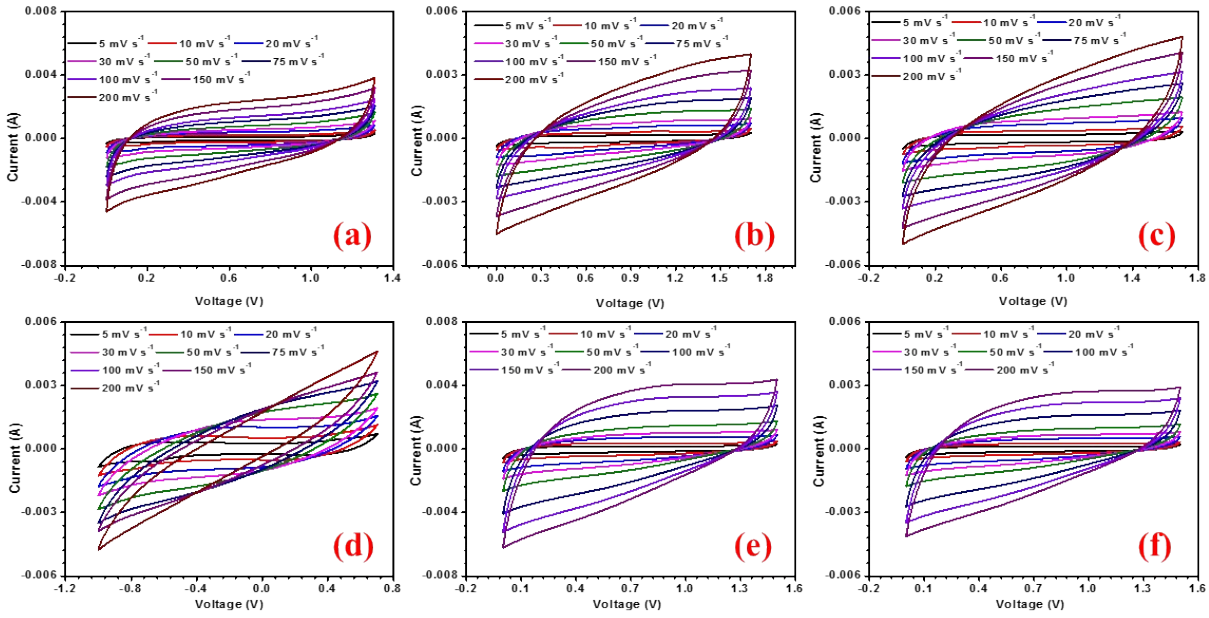

Fig. S15 CV curves at various scan rate for (a) activated carbon, (b) carbon microsphere, (c) carbon nanosphere, (d) graphene oxide and (e) graphene quantum dot and (f) nitrogen doped graphene quantum dot.

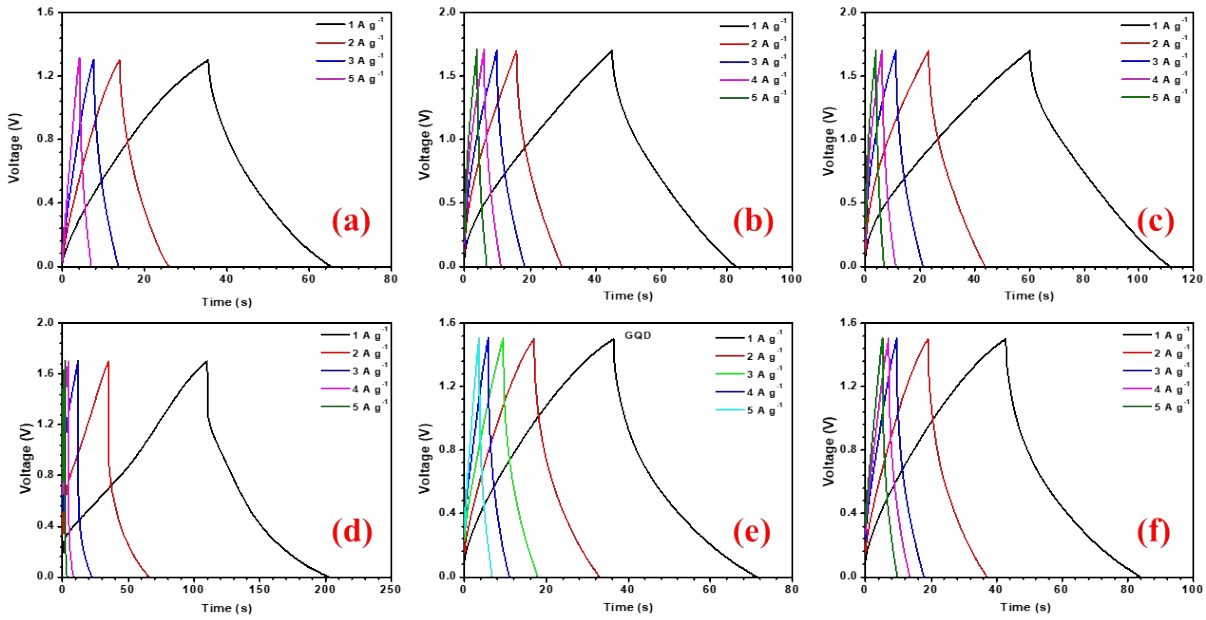

Fig. S16 CD curves at various scan rate for device of $NaFePO_4$ with (a) activated carbon, (b) carbon microsphere, (c) carbon nanosphere, (d) graphene oxide and (e) graphene quantum dot and (f) nitrogen doped graphene quantum dot.

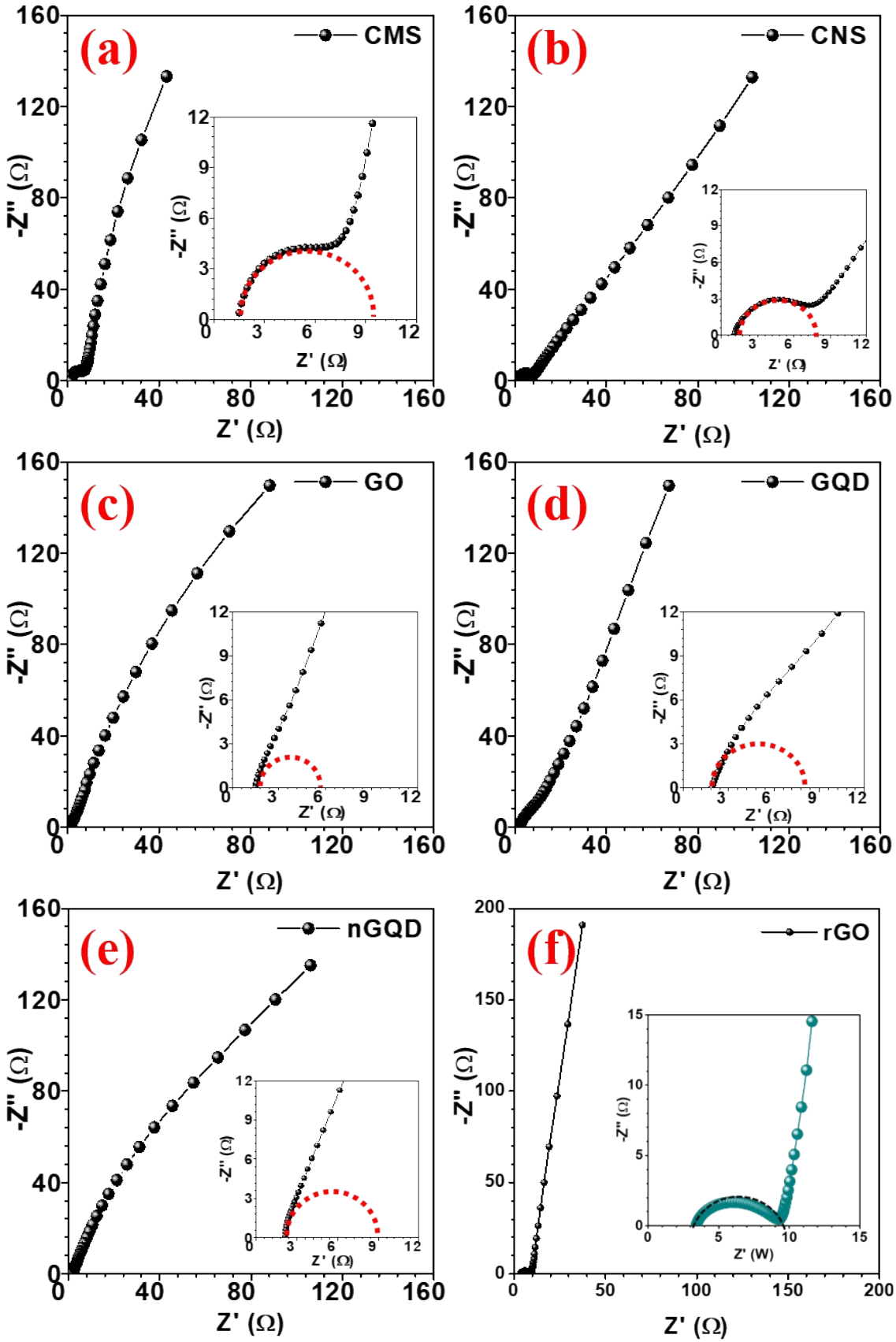

Fig. S17 EIS spectroscopy study of All the asymmetric devices.

Table S4. Energy and power density for different NFP and carbonaceous combinations at different current densities.

Energy density: E (W h kg^{-1})

Power density: P (W kg^{-1})

Current density (A g^{-1})	**AC**		**CMS**		**CNS**		**GO**		**RGO**		**GQD**		**NGQD**	
	E	**P**	**E**	**P**	**E**	**P**	**E**	**P**	**E**	**P**	**E**	**P**	**E**	**P**
1	5.40	659.0	9.23	878.1	13.84	896.6	15.71	628.3	25.29	894.3	7.81	803.8	9.38	822.6
2	4.69	1417.8	7.22	1895.8	10.43	1815.0	14.44	1638.9	23.68	1889.5	7.50	1704.5	8.44	1694.1
3	3.52	2057.6	6.42	2782.2	7.63	2821.7	10.24	2330.3	22.48	3381.5	6.56	2836.1	7.50	2727.3
4	--	--	5.62	3958.9	5.62	4078.6	6.18	4809.0	18.06	5423.2	5.63	3978.4	6.88	3867.2
5	2.82	4466.9	3.61	5052.4	4.01	5265.2	4.33	5395.7	13.65	8161.1	4.69	5408.6	6.25	5090.5